

A Slope Stability Model for Spatially Random Soils

Gordon A. Fenton

Dalhousie University, Halifax, NS B3J 2X4, Gordon.Fenton@dal.ca

D. V. Griffiths

Colorado School of Mines, Golden, CO 80401, D.V.Griffiths@mines.edu

Anthony Urquhart

Dalhousie University, Halifax, NS B3J 2X4

Keywords: slope stability, reliability, spatial variability

ABSTRACT: It is well known that slope stability reliability analyses are complicated by spatial variation in soil properties. This paper presents the results of a random finite element method (RFEM) analysis of a slope in which the soil is represented by a spatially random field and slope stability is evaluated using the finite element method. A significant advantage to the finite element method in slope stability calculations is that it allows the failure surface to find the weakest path through the soil. The paper investigates the resulting slope failure probability, as a function of the soil's statistical parameters, and proposes a simplified harmonic averaging approach to estimating the failure probability that avoids the necessity for Monte Carlo simulation of the slope.

1 INTRODUCTION

The failure prediction of a soil slope has been a long-standing geotechnical problem, and one which has attracted a wide variety of solutions. Traditional approaches to the problem generally involve assuming that the soil slope is homogeneous (spatially constant), or possibly layered, and techniques such as Taylor's (1937) stability coefficients for frictionless soils, the method of slices, and other more general methods involving arbitrary failure surfaces have been developed over the years. The main drawback to these methods is that they are not able to easily find the critical failure surface in the event that the soil properties are spatially varying.

In the realistic case where the soil properties vary randomly in space, the slope stability problem is best captured via a non-linear finite element model which has the distinct advantage of allowing the failure surface to seek out the path of least resistance. In this paper such a model is employed, which, when combined with a random field simulator, allows the realistic probabilistic evaluation of slope stability. This work is a follow up of the analysis by Griffiths and Fenton (2000) and considers the same soil slope problem. The slope is assumed to be an undrained clay, with $\phi_u = 0$, of height H with a 2:1 gradient resting on a foundation layer, also of depth H . The finite element mesh is shown in Figure 1.

The soil is represented by a random spatially varying undrained cohesion field, $c_u(\underline{x})$, which is assumed to be lognormally distributed, where \underline{x} is the spatial position. The cohesion has mean, μ_{c_u} , standard deviation, σ_{c_u} and is assumed to have an exponentially decaying (Markovian) correlation structure,

$$\rho_{\ln c_u}(\tau) = e^{-2|\tau|/\theta_{\ln c_u}} \quad (1)$$

where τ is the distance between two points in the field. Note that the correlation structure has been assumed

isotropic in this study. The use of an anisotropic correlation is straightforward, within the framework developed here, but is a site specific extension which does not particularly contribute to the overall understanding of the stochastic nature of the problem.

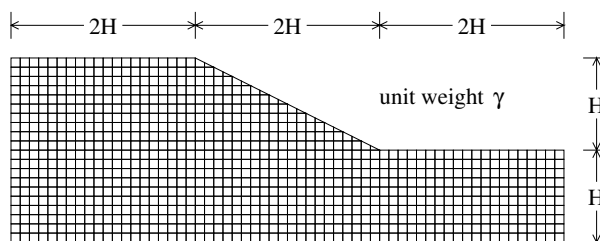


Figure 1. Mesh used for slope stability analysis.

The correlation function has a single parameter, $\theta_{\ln c_u}$, the correlation length. Because c_u is assumed to be lognormally distributed, its logarithm, $\ln c_u$, is normally distributed. The correlation function is measured in this study relative to the underlying normally distributed field. Thus, $\rho_{\ln c_u}(\tau)$ gives the correlation coefficient between $\ln c_u$ at two points in the field separated by a distance τ . In practice, the parameter $\theta_{\ln c_u}$ is estimated from spatially distributed c_u samples by using the logarithm of the samples rather than the raw data themselves. If the actual correlation between points in the c_u field is desired, the following transformation can be used (Vanmarcke, 1984),

$$\rho_{c_u}(\tau) = \frac{\exp\{\rho_{\ln c_u}(\tau)\sigma_{\ln c_u}^2\} - 1}{\exp\{\sigma_{\ln c_u}^2\} - 1} \quad (2)$$

Since $\theta_{\ln c_u}$ is a length, it can be non-dimensionalized by dividing it by H , a measure of the embankment size. Thus, the results given here can be applied to any size problem, so long as it has the same slope and

same depth to height ratio. The standard deviation, σ_{c_u} may also be expressed in terms of the dimensionless coefficient of variation

$$V = \frac{\sigma_{c_u}}{\mu_{c_u}} \quad (3)$$

If the mean and variance of the underlying $\ln c_u$ field are desired, they can be obtained through the transformations

$$\sigma_{\ln c_u}^2 = \ln(1 + V^2), \quad \mu_{\ln c_u} = \ln(\mu_{c_u}) - \frac{1}{2}\sigma_{\ln c_u}^2 \quad (4)$$

By using Monte Carlo simulation, where the soil slope is simulated and analyzed by the finite element method repeatedly, estimates of the probability of failure are obtained over a range of soil statistics. The failure probabilities are compared to those obtained using a harmonic average of the cohesion field employed in Taylor's stability coefficient method and very good agreement is found. The study indicates that the stability of a spatially varying soil slope is well modeled using a harmonic average of the soil properties.

2 THE RANDOM FINITE ELEMENT MODEL

The slope stability analyses use an elastic-perfectly plastic stress-strain law with a Tresca failure criterion. Plastic stress redistribution is accomplished using a viscoplastic algorithm which uses 8-node quadrilateral elements and reduced integration in both the stiffness and stress redistribution parts of the algorithm. The theoretical basis of the method is described more fully in Chapter 6 of the text by Smith and Griffiths (1998), and for a discussion of the method applied to slope stability analysis, the reader is referred to Griffiths and Lane (1999) and Paice and Griffiths (1997).

In brief, the analyses involve the application of gravity loading, and the monitoring of stresses at all the Gauss points. If the Tresca criterion is violated, the program attempts to redistribute those stresses to neighboring elements that still have reserves of strength. This is an iterative process which continues until the Tresca criterion and global equilibrium are satisfied at all points within the mesh under quite strict tolerances.

In this study, "failure" is said to have occurred if, for any given realization, the algorithm is unable to converge within 500 iterations. Following a set of 2000 realizations of the Monte-Carlo process the probability of failure is simply defined as the proportion of these realizations that required 500 or more iterations to converge.

While the choice of 500 as the iteration ceiling is subjective, Griffiths and Fenton (2000) found that the probability of failure computed using this criterion is quite stable even for as few as 200 iterations.

The random finite element model (RFEM) combines the deterministic finite element analysis with a random field simulator, which, in this study, is the Local Average Subdivision (LAS) method developed by Fenton

and Vanmarcke (1990). The LAS algorithm produces a field of random element values, each representing a local average of the random field over the element domain, which are then mapped directly to the finite elements. The random elements are local averages of the log-cohesion, $\ln c_u$, field. The resulting realizations of the log-cohesion field have correlation structure and variance correctly accounting for local averaging over each element. Much discussion of the relative merits of various methods of representing random fields in finite element analysis has been carried out in recent years (see, for example, Li and Der Kiureghian, 1993). While the spatial averaging discretization of the random field used in this study is just one approach to the problem, it is appealing in the sense that it reflects the simplest idea of the finite element representation of a continuum as well as the way that soil samples are typically taken and tested in practice, ie. as local averages. Regarding the discretization of random fields for use in finite element analysis, Matthies et al. (1997) makes the comment that "One way of making sure that the stochastic field has the required structure is to assume that it is a local averaging process.", referring to the conversion of a nondifferentiable to a differentiable (smooth) stochastic process. Matthie further goes on to say that the advantage of the local average representation of a random field is that it yields accurate results even for rather coarse meshes.

Figure 2 illustrates two possible realizations arising from the RFEM. In this figure, dark regions correspond to weaker soil. Notice how convoluted the failure region is, particularly at the smaller scale of fluctuation. In addition, it can be seen that the slope failure involves the plastic deformation of an entire region above a vaguely defined failure 'surface'. Thus, failure is more complex than just a rigid 'circular' region sliding along a clearly defined interface as is typically assumed.

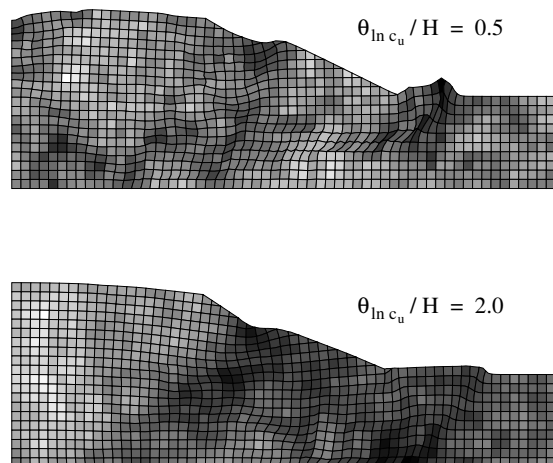


Figure 2. Two typical failed random field realizations. Low strength regions are dark.

3 PARAMETRIC STUDIES

To keep the study non-dimensional, the mean soil strength is expressed in the form of a mean dimensionless shear strength,

$$\mu_{N_s} = \frac{\mu_{c_u}}{\gamma H} \quad (5)$$

where γ is the unit weight of the soil. In the case where the cohesion field is everywhere the same and equal to μ_{c_u} , a value of $\mu_{N_s} = 0.17$ corresponds to a factor-of-safety, $F = 1.0$, which is to say that the slope is on the verge of failure.

This study considers the following values of the input statistics, μ_{N_s} , $\theta_{\ln c_u}/H$, and V ;

$$\begin{aligned} \mu_{N_s} &= 0.15, 0.17, 0.20, 0.25, 0.30 \\ \theta_{\ln c_u}/H &= 0.10, 0.20, 0.50, 1.00, 2.00, 5.00, 10.0 \\ V &= 0.10, 0.20, 0.50, 1.00, 2.00, 5.00 \end{aligned}$$

For each set of the above parameters, 2000 realizations of the soil field were simulated and analyzed, from which the probability of slope failure was estimated. The detailed probability estimates are presented in Griffiths and Fenton (2000). In this paper only the estimated failure probabilities are presented (see Figure 6) and compared to those predicted using the harmonic average model.

4 SEMI-THEORETICAL MODEL

In Taylor's stability coefficient approach to slope stability, the coefficient

$$N_s = \frac{c_u}{\gamma H} \quad (6)$$

assumes that the soil is completely uniform, having cohesion equal to c_u everywhere. This coefficient may then be compared to the critical coefficient obtained from Taylor's charts to determine if slope failure will occur or not. For the slope geometry studied here, slope failure will occur if $N_s < 0.17$.

In the case where c_u is randomly varying in space, two issues present themselves. First of all Taylor's method cannot be used on a non-uniform soil and secondly Eq. (6) now includes a random quantity on the right-hand-side (namely, $c_u = c_u(\underline{x})$) so that N_s becomes random. The first issue can be solved by finding some representative value of c_u , which will be referred to here as \bar{c}_u , such that the stability coefficient method still holds. That is, \bar{c}_u would be the cohesion of a uniform soil such that it has the same slope stability as the real spatially varying soil.

The question now is, how should this effective soil cohesion value be defined? First of all, each soil realization will have a different value of \bar{c}_u , so that Eq. (6) is still a function of a random quantity, namely,

$$N_s = \frac{\bar{c}_u}{\gamma H} \quad (7)$$

and, if the distribution of \bar{c}_u is found, the distribution of N_s can be derived. The failure probability of the slope then becomes equal to the probability that N_s is less than the Taylor critical value of 0.17.

This line of reasoning suggests that \bar{c}_u should be defined as some sort of average of c_u over the soil domain where failure is occurring. Three common types of averages present themselves;

- 1) *Arithmetic average*: the arithmetic average over some domain, A , is defined as,

$$\bar{X}_a = \frac{1}{n} \sum_{i=1}^n c_{u_i} = \frac{1}{A} \int_A c_u(\underline{x}) d\underline{x} \quad (8)$$

for the discrete and continuous cases, where the domain A is assumed to be divided up into n samples in the discrete case. The arithmetic average weights all of the values of c_u equally. In that the failure surface seeks a path through the weakest parts of the soil, this form of averaging is not deemed to be appropriate for this problem.

- 2) *Geometric average*: the geometric average over some domain, A , is defined as,

$$\bar{X}_g = \left(\prod_{i=1}^n c_{u_i} \right)^{1/n} = \exp \left\{ \frac{1}{A} \int_A \ln c_u(\underline{x}) d\underline{x} \right\} \quad (9)$$

The geometric average is dominated by low values of c_u and, for a spatially varying cohesion field, will always be less than the arithmetic average. This average potentially reflects the reduced strength as seen along the failure path and has been found by the authors (Fenton and Griffiths, 2002 and 2003) to well represent the bearing capacity and settlement of footings founded on spatially random soils. The geometric average also is a 'natural' average of the lognormal distribution, since an arithmetic average of the underlying normally distributed random variable, $\ln c_u$, leads to the geometric average when converted back to the lognormal distribution. Thus, if c_u is lognormally distributed, its geometric local average is also lognormally distributed.

- 3) *Harmonic average*: the harmonic average over some domain, A , is defined as,

$$\bar{X}_h = \left[\frac{1}{n} \sum_{i=1}^n \frac{1}{c_{u_i}} \right]^{-1} = \left[\frac{1}{A} \int_A \frac{d\underline{x}}{c_u(\underline{x})} \right]^{-1} \quad (10)$$

This average is even more influenced by small values than is the geometric average. In general, for a spatially varying random field, the harmonic average will be smaller than the geometric average, which in turn is smaller than the arithmetic average. Unfortunately, the mean and variance of

the harmonic average, for a spatially correlated random field, are not easily found.

Putting aside for the moment the issue of how to compute the effective undrained cohesion, \bar{c}_u , the averaging domain must also be determined. This should be approximately equal to the area of the soil which fails during a slope failure. It is expected that the value of \bar{c}_u will change slowly with changes in the averaging area, and so only an approximate area need be determined. The area selected for this model is a parallelogram, as shown in Figure 3, having slope length equal to the length of the slope and horizontal surface length equal to H . For the purposes of computing the average, it is further assumed that this area can be approximated by a rectangle of dimension $w \times h$ (the *variance function* which gives the variance reduction after local averaging is commonly defined on a rectangle). As far as the local averaging is concerned, the parallelogram and rectangle will have practically the same local averages and, thus, the same statistics.

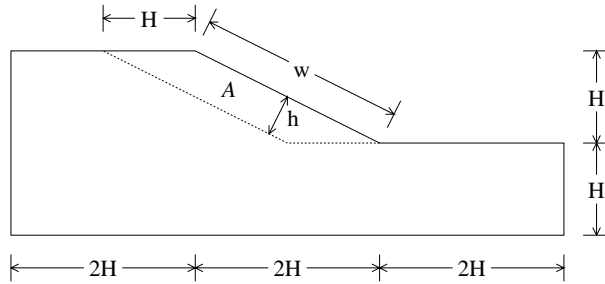


Figure 3. Assumed averaging domain.

The values of w and h are

$$w = H / \sin \beta, \quad h = H \sin \beta \quad (11)$$

such that $w \times h = H^2$, where β is the slope angle (in this case 26.6°). It appears, when comparing Figure 2 to Figure 3, that the assumed averaging domain of Figure 3 is smaller than the deformed regions seen in Figure 2. A general prescription for the size of the averaging domain is not yet known, although it should capture the approximate area of the soil involved in resisting the slope deformation. The area assumed in Figure 3 is to be viewed as an initial approximation which, as will be seen, yields reasonably good results. A considerably expanded parametric study, including different slope geometries, needs to be performed to resolve the issue.

With an assumed averaging domain, $A = w \times h$, the geometric average leads to the following definition for \bar{c}_u ,

$$\bar{c}_u = \bar{X}_g = \exp \left\{ \frac{1}{A} \int_A \ln c_u(\underline{x}) d\underline{x} \right\} \quad (12)$$

which, if c_u is lognormally distributed, is also lognormally distributed. The resulting coefficient

$$N_s = \frac{\bar{c}_u}{\gamma H} \quad (13)$$

is then also lognormally distributed with mean and variance

$$\mu_{\ln N_s} = \mu_{\ln c_u} - \ln(\gamma H) \quad (14a)$$

$$\sigma_{\ln N_s}^2 = \sigma_{\ln c_u}^2 = \gamma(w, h) \sigma_{\ln c_u}^2 \quad (14b)$$

The function $\gamma(w, h)$ is the so-called variance function which lies between 0 and 1 and gives the amount that the variance of a local average is reduced from the point value. It is formally defined as the average of correlations between every pair of points in the averaging domain,

$$\gamma(w, h) = \frac{1}{A^2} \int_A \int_A \rho(\xi - \eta) d\xi d\eta \quad (15)$$

Solutions to this integral, albeit sometimes approximate, exist for most common correlation functions.

The probability of failure, p_f , can now be computed by assuming that Taylor's stability coefficient method holds when using this effective value of cohesion, namely by computing

$$p_f = P[N_s < N_{crit}] = \Phi \left(\frac{\ln N_{crit} - \mu_{\ln N_s}}{\sigma_{\ln N_s}} \right) \quad (16)$$

where the critical stability coefficient for the slope considered is $N_{crit} = 0.17$ and Φ is the cumulative distribution function for the standard normal. These values of failure probability can then be compared to those obtained via simulation.

The geometric average for \bar{c}_u generally led to predicted failure probabilities which significantly underestimated the probabilities determined via simulation and changes in the averaging domains size did not particularly improve the prediction. This means that the soil strength as 'seen' by the finite element model was even lower, in general, than that predicted by the geometric average. Thus, the geometric average was abandoned as the correct measure for \bar{c}_u .

Since the harmonic average yields values which are even lower than the geometric average, the harmonic average over the same domain, $A = w \times h$, is now investigated as representative of \bar{c}_u , namely,

$$\bar{c}_u = \bar{X}_h = \left[\frac{1}{A} \int_A \frac{d\underline{x}}{c_u(\underline{x})} \right]^{-1} \quad (17)$$

Unfortunately, so far as the authors are aware, no relatively simple expressions exist for the moments of \bar{c}_u , as defined above, for a spatially correlated random field. The authors are continuing research on this problem but, for the time being, these moments can be obtained by simulation. It may seem questionable to be developing a probabilistic model with the nominal goal of eliminating the necessity of simulation, when that model still requires simulation. However, the moments of the harmonic mean can be arrived at in a small fraction of the time taken to perform the non-linear slope stability simulation.

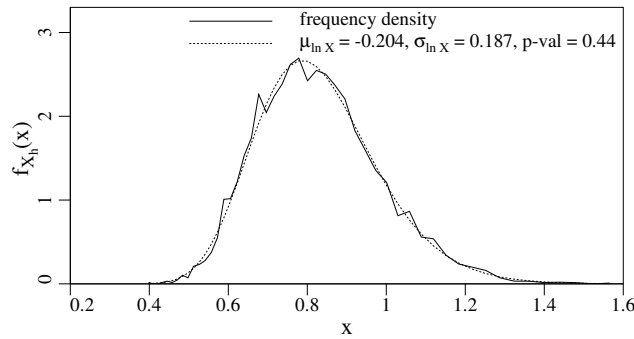


Figure 4. Histogram of harmonic averages along with fitted lognormal distribution.

In order to compute probabilities using the statistics of \bar{c}_u , it is necessary to know the distribution of $N_s = \bar{c}_u/(\gamma H)$. For lognormally distributed c_u , the distribution of the harmonic average is not simple. However, since \bar{c}_u is strictly non-negative ($c_u \geq 0$), it seems reasonable to suggest that \bar{c}_u is at least approximately lognormal. A histogram of the harmonic averages obtained in the case where $V = 0.5$ and $\theta_{\ln c_u}/H = 0.5$ is shown in Figure 4, along with a fitted lognormal distribution. The p-value for the Chi-Square goodness-of-fit test is 0.44, indicating that the lognormal distribution is very reasonable, as also indicated by the plot. Similar results were obtained for other parameter values.

The procedure to estimate the mean and variance of the harmonic average, \bar{c}_u , for each parameter set (μ_{N_s} , V , and $\theta_{\ln c_u}/H$) considered in this study involves; a) generating a large number of random cohesion fields, each of dimension $w \times h$, b) computing the harmonic average of each using Eq. (10), and c) estimating the mean and variance of the resulting set of harmonic averages. Using 5000 random field realizations, the resulting estimates for the mean and standard deviation of $\ln \bar{X}_h$ are shown in Figure 5 for random fields with mean 1.0. Since \bar{c}_u is assumed to be (at least approximately) lognormally distributed, having parameters $\mu_{\ln \bar{c}_u}$ and $\sigma_{\ln \bar{c}_u}$, the mean and standard deviation of the logarithm of the harmonic averages are shown in Figure 5.

The slope failure probability can now be computed as in Eq. (16),

$$p_f = P[N_s < N_{crit}] = \Phi \left(\frac{\ln N_{crit} - \mu_{\ln N_s}}{\sigma_{\ln N_s}} \right) \quad (18)$$

except that now the mean and standard deviation of $\ln N_s$ are computed using the harmonic mean results of Figure 5, suitably scaled for the actual value of $\mu_{c_u}/\gamma H$,

$$\mu_{\ln N_s} = \ln(\mu_{c_u}/\gamma H) + \mu_{\ln \bar{x}_h} = \ln(\mu_{N_s}) + \mu_{\ln \bar{x}_h} \quad (19a)$$

$$\sigma_{\ln N_s} = \sigma_{\ln \bar{x}_h} \quad (19b)$$

where $\mu_{\ln \bar{x}_h}$ and $\sigma_{\ln \bar{x}_h}$ are read from Figure 5, given the scale of fluctuation and coefficient of variation.

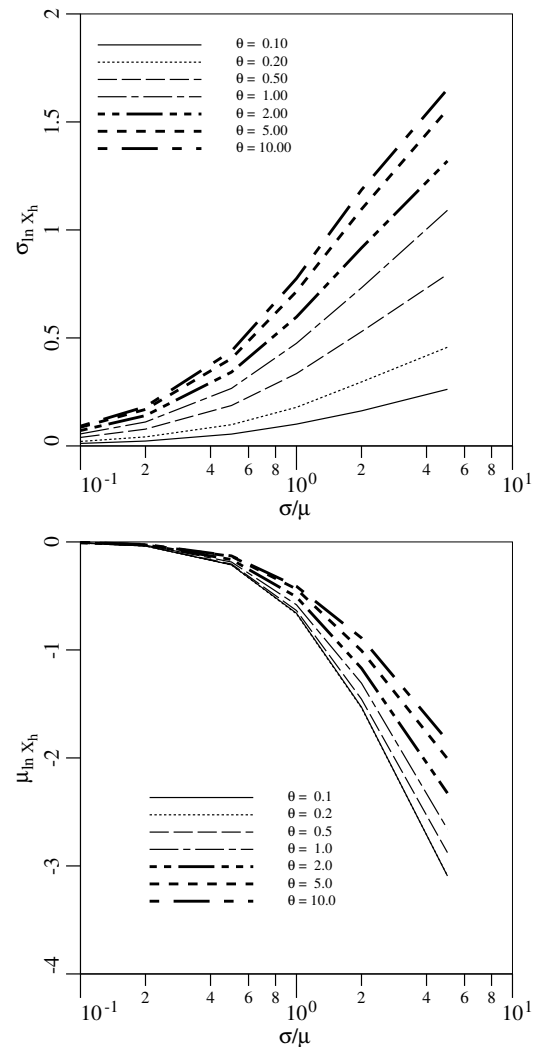


Figure 5. Mean and standard deviation of log-harmonic averages estimated from 5000 simulations.

Figure 6 shows the predicted failure probabilities versus the failure probabilities obtained via simulation over all parameter sets considered. The agreement is remarkably good, considering the fact that the averaging domain was rather arbitrarily selected, and there was no a-priori evidence that the slope stability problem should be governed by a harmonic average. The results of Figure 6 indicate that the harmonic average gives a good probabilistic model of slope stability.

There are two outliers in Figure 6 where the predicted failure probability considerably overestimates that obtained via simulation. These correspond to the cases where 1) $\mu_{N_s} = 0.3$, $V = 1.0$ and $\theta_{\ln c_u}/H = 0.1$ (simulated probability is 0.047 versus predicted probability of 0.82) and 2) $\mu_{N_s} = 0.3$, $V = 1.0$ and $\theta_{\ln c_u}/H = 0.2$ (simulated probability is 0.31 versus predicted probability of 0.74). Both cases correspond to the largest factor of safety considered in the study ($\mu_{N_s} = 0.3$ gives a factor of safety of 1.77 in the uniform soil case). Also the small scales of fluctuation yield the smallest values of $\sigma_{\ln N_s}$ which, in turn, implies that

the cumulative distribution function of $\ln N_s$ increases very rapidly over a small range. Thus, slight errors in the estimate of $\mu_{\ln N_s}$ makes for large errors in the probability. For example, the worst case seen in Figure 6 has predicted values of

$$\begin{aligned}\mu_{\ln N_s} &= \ln(\mu_{N_s}) + \mu_{\ln \bar{x}_h} = \ln(0.3) - 0.66 = -1.864 \\ \sigma_{\ln N_s} &= \sigma_{\ln \bar{x}_h} = 0.10\end{aligned}$$

The predicted failure probability is thus

$$\begin{aligned}P[N_s < 0.17] &= \Phi\left(\frac{\ln 0.17 + 1.864}{0.10}\right) = \Phi(0.92) \\ &= 0.82\end{aligned}$$

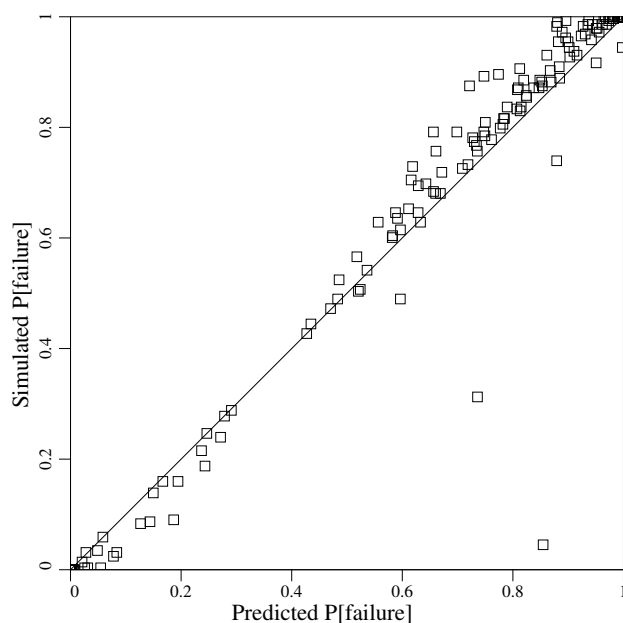


Figure 6. Simulated failure probabilities versus failure probabilities predicted using a harmonic average of c_u over domain $w \times h$.

A relatively small error in the estimation of $\mu_{\ln N_s}$ can lead to a large change in probability. For example, if $\mu_{\ln N_s}$ was -1.60 instead of -1.864 , a 14% change, then the predicted failure probability becomes

$$\begin{aligned}P[N_s < 0.17] &= \Phi\left(\frac{\ln 0.17 + 1.6}{0.10}\right) = \Phi(-1.72) \\ &= 0.043\end{aligned}$$

which is about what was obtained via simulation. For small values of $\theta_{\ln c_u}/H$ and other coefficients of variation, the failure probability tends to be either close to zero ($V < 1.0$) or close to 1.0 ($V > 1.0$), in which case the predicted and simulated probabilities are in much better agreement. The conclusion that can be drawn from these two outliers is that the harmonic average model is not a perfect predictor in the region where the cumulative distribution is rapidly increasing. However, in these cases, the predicted failure

probability is over-estimated, which is at least conservative. Further study is required to see if the probability prediction can be refined by using a different averaging domain.

For all other results, especially where the factor of safety is closer to 1.0 ($\mu_{N_s} < 0.3$), the harmonic average model leads to very good estimates of failure probability. In particular, for small failure probabilities, the predicted failure probability is generally conservative, slightly overestimating the failure probability.

5 CONCLUSIONS

This study considers just one possible geometry for an undrained clay slope. Nevertheless, the results are instructive. The basic idea pursued here is that the Taylor stability coefficients can still be used for a soil with spatially varying properties so long as an ‘effective’ soil property is found to represent the slope. A property which closely captures the slope failure probability was found to be the harmonic average of c_u over a domain of size $w \times h$. The harmonic average is dominated by low strength regions appearing in the soil slope, which agrees with how the failure surface will seek out the low strength areas.

The averaging region used to characterize the slope stability problem is still an area requiring additional research. While preliminary simulation studies by the authors indicate that the results are not particularly sensitive to the actual size of the area used, the area should be related to the slope geometry under consideration. In addition, simplified moments of the harmonic average for a spatially correlated random field are needed.

One important observation arising from this study is that soil slopes appear to be well characterized by computing a harmonic average of soil sample values, rather than by using an arithmetic average, as is done traditionally. That is, the reliability of an existing slope can be estimated by sampling the soil at a number of locations in the slope, computing the harmonic average of the sample values, and then applying Taylor’s stability coefficient approach to assess the factor-of-safety.

6 REFERENCES

- Fenton, G.A. and Griffiths, D.V. (2002). “Probabilistic Foundation Settlement on Spatially Random Soil,” *ASCE J. Geotech. Geoenv. Eng.*, **128**(5), 381–390.
- Fenton, G.A. and Griffiths, D.V. (2003). “Bearing Capacity of Spatially Random $c - \phi$ Soils,” *Can. Geotech. J.*, **40**(1), 54–65.
- Fenton, G.A. and Vanmarcke, E.H. (1990). “Simulation of Random Fields via Local Average Subdivision,” *ASCE J. Engrg. Mech.*, **116**(8), 1733–1749.
- Griffiths, D.V. and Fenton, G.A. (2000). “Influence of soil strength spatial variability on the stability of an undrained clay slope by finite elements,” *ASCE Geotechnical Special Publication No. 101*, 184–193.
- Griffiths, D.V. and Lane, P.A. (1999). “Slope stability analysis by finite elements,” *Géotechnique*, **49**(3), 387–403.
- Li, C.-C. and Der Kiureghian, A. (1993). “Optimal discretization of random fields,” *ASCE J. Engrg. Mech.*, **119**(6), 1136–1154.
- Matthies, H.G., Brenner, C.E., Bucher, C.G. and Soares, C.G. (1997). “Uncertainties in probabilistic numerical analysis of structures and solids – stochastic finite elements,” *Structural Safety*, **19**(3), 283–336.
- Paice, G.M. and Griffiths, D.V. (1997). “Reliability of an undrained clay slope formed from spatially random soil,” *IACMAG 97, A.A. Balkema*, Yuan, J.-X., ed., Rotterdam, 1205–1209.
- Smith, I.M. and Griffiths, D.V. (1998). *Programming the Finite Element Method*, ((3rd Ed.)), John Wiley & Sons, New York, NY.
- Taylor, D.W. (1937). “Stability of earth slopes,” *Journal of the Boston Society of Civil Engineers*, **24**(3), 337–386.
- Vanmarcke, E.H. (1984). *Random Fields: Analysis and Synthesis*, The MIT Press, Cambridge, Massachusetts.